Proceedings of ICAD2011
The Sixth International Conference on Axiomatic Design
Daejeon – March 30-31, 2011
ICAD-2011-26

AXIOMATIC SYSTEM DESIGN FOR NON-THERMAL DICING OF QUARTZ WAFERS

Seunghwoi Han
ddelle@kaist.ac.kr
Precision Engineering & Metrology Lab
Department of Mechanical Engineering
Korea Advanced Institute of Science and Technology
373-1 Guseong-dong Yuseong-gu
305-701, Daejeon, South Korea

Yunseok Kim
kkyyss@kaist.ac.kr
Precision Engineering & Metrology Lab
Department of Mechanical Engineering
Korea Advanced Institute of Science and Technology
373-1 Guseong-dong Yuseong-gu
305-701, Daejeon, South Korea

Young-Jin Kim
yj.kim@kaist.ac.kr
Precision Engineering & Metrology Lab
Department of Mechanical Engineering
Korea Advanced Institute of Science and Technology
373-1 Guseong-dong Yuseong-gu
305-701, Daejeon, South Korea

Seungman Kim
kimsm@kaist.ac.kr
Precision Engineering & Metrology Lab
Department of Mechanical Engineering
Korea Advanced Institute of Science and Technology
373-1 Guseong-dong Yuseong-gu
305-701, Daejeon, South Korea

Sanguk Park
telemach@kaist.ac.kr
Precision Engineering & Metrology Lab
Department of Mechanical Engineering
Korea Advanced Institute of Science and Technology
373-1 Guseong-dong Yuseong-gu
305-701, Daejeon, South Korea

Jiyong Park
j-park@kaist.ac.kr
Precision Engineering & Metrology Lab
Department of Mechanical Engineering
Korea Advanced Institute of Science and Technology
373-1 Guseong-dong Yuseong-gu
305-701, Daejeon, South Korea

Seung-Woo Kim
swk@kaist.ac.kr
Precision Engineering & Metrology Lab
Department of Mechanical Engineering
Korea Advanced Institute of Science and Technology
373-1 Guseong-dong Yuseong-gu
305-701, Daejeon, South Korea

ABSTRACT

In the manufacture of light emitting diodes (LEDs), the process of dicing that separates fabricated chips into pieces from quartz wafers is critically important as it determines the quality and productivity of produced LEDs. However, traditional methods using either mechanical grinding wheels or relatively long pulse lasers suffers mechanical or thermal defects such as debris, cracks, heat-affected zone and large dicing width. In this work, an axiomatic design approach is used to develop a novel high-brightness wafer dicing machine that allows minimized mechanical thermal effects with the aid of ultrafast femtosecond laser pulses.

Keywords: wafer dicing, femtosecond pulse laser, non-thermal machining.

1 INTRODUCTION

Since 2000, the market for LEDs has grown at an average annual rate over 9.0 % to reach a value of 1.6 billion USD in 2008. This growth has been driven by the novel emerging market of flat panel displays, automotive, signage, and the amusement and lighting industry. As the whole market size increases, the improvement of the overall manufacturing process is getting more critical to meet the customer's diverse requirements. The LED manufacturing process consists of four steps, epi wafer manufacturing, chip production, packaging, module, in order. In chip production, the separation of fabricated chips into pieces is one of the most important procedures for high brightness LEDs, which is the so called wafer dicing process. Here, we present an overall design process of the LED wafer dicing machine based on the axiomatic design approach [Suh, 2001].

2 CNS, FRS AND FEMTOSECOND LASER MACHINING

First, it is essential to define customer's needs (CNs) for the design of the LED wafer dicing machine. The customer here is the LED manufacturer and representative CNs for LED products are: 'high brightness' and 'high productivity'. In terms of the brightness, mechanical and thermal defects of wafer dicing such as debris, cracks, and heat affected zones

(HAZs) severely limit the LED performance which stems from the melting process of the target material. Therefore we can set the main functional requirement (FR) to 'dice the wafer' and then set the first sub-FR to 'decrease the thermal effects'. High productivity can be realized by 'increasing the dicing speed', the second sub-FR.

These two sub-FRs are not easy to satisfy at the same time due to the limitations of conventional dicing methods. Mechanical grinding makes unwanted vibration and high temperatures which result in residual stress, debris, cracks, and HAZs on the LED wafer even though it offers high speed. Vibration and thermal effects can be partially decreased by using continuous or pulse lasers, which are not, however, still sufficient level. A novel non-thermal laser dicing method is adopted here by using high-peak power of ultrafast femtosecond (fs, $1/10^{15}$ s) pulses for LED wafers. Unlike conventional thermal laser dicing, femtosecond pulses directly convert the target material into plasma without a temperature induced phase change from solid to liquid or vapour. This enables non-thermal dicing of the LED wafer without any performance degradation as shown in Figure 1. Confined energy in ultra-short time duration would also enable high productivity. An axiomatic design approach is made to develop a novel LED dicing machine here with the aid of ultrafast femtosecond laser pulses.

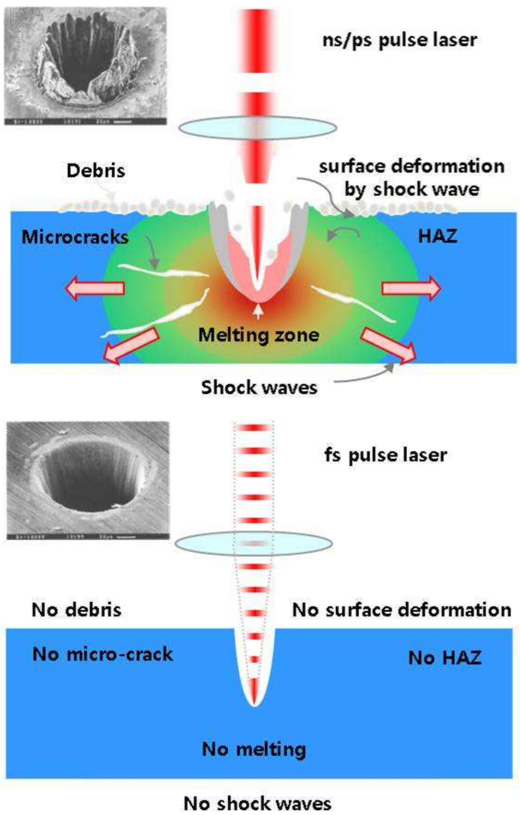

Figure 1. Non-thermal fabrication using ultrafast femtosecond laser pulses.

3 DPS OF NEW DICING MACHINE

The four domains of design are as shown in Figure 2: the customer domain, functional domain, physical domain and process domain. CNs and FRs are defined as above. Now it is time to define design parameters (DPs) and process variables (PVs). DPs are qualitative and quantitative aspects of physical and functional characteristics of the LED dicing machine, which can be defined through the interaction between the fs laser pulse and LED wafer.

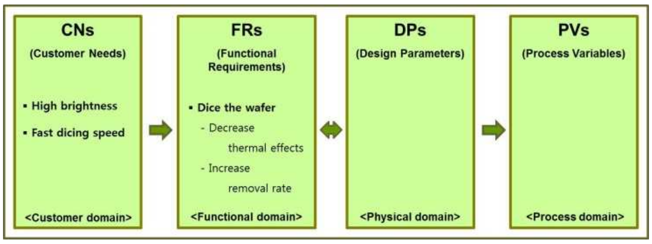

Figure 2. The four domains of design.

3.1 THE INTERACTION BETWEEN ULTRAFAST FEMTOSECOND LASER PULSE AND MATERIAL

To remove atoms or molecules from a target material by laser pulses, one should deliver energy well over the binding energy of the target atom or molecule. This kind of removal phenomenon in excess of the binding energy is called ablation, and it can be analysed by a two-temperature model (TTM) [Chichkov *et al.*, 1996]. The ultra-short pulse irradiated material is divided into two sub systems for the TTM analysis: the electron sub-system and lattice sub-system. The TTM defines the whole ablation procedure into three steps: electron ionization, heat transfer from electron to lattice, and ion separation. The detailed study for each process is required to determine the DPs. When ultra-short pulses are irradiated to a target material, the energy is firstly absorbed by electron sub-system. Then, energetic electrons escape from the parent material, which is called ionization. There are two ionization mechanism, photo-ionization and avalanche ionization, which usually occur at the same time.

The photo-ionization is a direct excitation of electrons by the irradiated laser field. It can be further divided into tunnelling ionization and the multi-photon ionization (MPI). The former is caused by Coulomb well suppression in case of the ambient electric field being strong enough to free the bound electrons over the suppressed barrier. The latter is based on the absorption of several photons with relatively weak electric field by a single electron. The probabilities of these two photo-ionization processes depend on Keldysh parameter (γ) as shown in Figure 3.

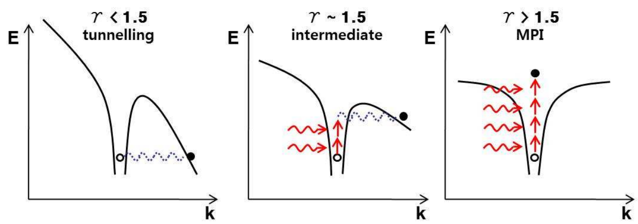

Figure 3. Photo-ionization process [Schaffer *et al.*, 2001].

The Keldysh parameter is a quantitative indicator of the regime which process might dominate the ionization and defined as follows [Schaffer *et al.*, 2001].

$$\gamma = \frac{\omega}{e}\left[\frac{mcn\varepsilon_0 E_g}{I}\right]^{1/2} \quad (1)$$

where, ω is the laser frequency, $\boldsymbol{m}$ is the reduced mass of the electron, $\boldsymbol{e}$ is the charge of the electron, $\boldsymbol{I}$ is the intensity of laser at focal point, $\boldsymbol{c}$ is the velocity of light, $\boldsymbol{n}$ is the refractive index of material, $\boldsymbol{E_g}$ is the band-gap energy of material, and ε_0 is the permittivity of free space.

Avalanche ionization is a linear absorption process of free carriers that is followed by impact ionization. Free electrons in the target material linearly absorb several photons. As a result, their energy states move to higher ones in the conduction band. For both energy and momentum to be conserved, electrons should transfer their own momentum by absorbing/emitting phonons. As shown in Figure 4, electrons then ionize other electrons from the valence to conduction band in a collision manner, which is called impact ionization.

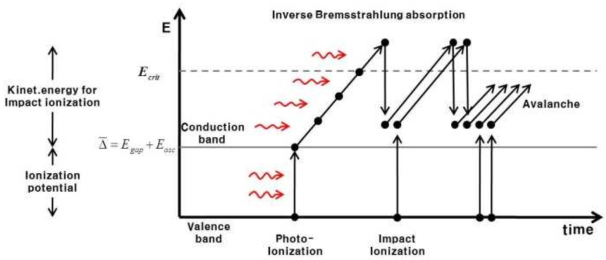

Figure 4. Avalanche ionization process.

The time dependent free electron density n_e can be expressed by the rate equation below [Gamaly *et al.*, 2002].

$$\frac{dn_e}{dt} = n_e w_{PI} + n_a w_{AI} \quad (2)$$

where, n_a is the density of neutral atoms, w_{PI} is the time independent probability for the photo-ionization and w_{AI} is the probability for the avalanche ionization. The probabilities w_{PI} and w_{AI} can be respectively written in the form

$$w_{PI} \approx \frac{\varepsilon_{osc}}{J_i}\left(\frac{2\omega^2 \nu_{eff}}{\omega^2 + \nu_{eff}^2}\right) \quad (3)$$

$$w_{AI} \approx \omega n_{ph}^{3/2}\left(\frac{\varepsilon_{osc}}{2J_i}\right)^{n_{ph}} \quad (4)$$

$$\varepsilon_{osc}[eV] = 9.3(1+\alpha^2)\frac{I}{10^{14}[W/cm^2]}(\lambda[\mu m])^2 \quad (5)$$

where ε_{osc} is the electron quiver energy in the laser field, $n_{ph} = J_i/\hbar\omega$ is the number of photons necessary for atom ionization by the multi-photon process, J_i is the ionization potential, ν_{eff} is the effective collision frequency, α accounts for the laser polarization, I is the peak power intensity of pulse laser and λ is the wavelength of laser.

The second step of the ablation mechanism is heat transfer from the electron to the lattice sub-system. The TTM which models heat transfer in a material as a function of space and time can be used for ultra-short laser pulses. Two sub-systems in TTM are governed by two coupled differential equations. Energy transfer from the electron to the lattice sub-system by Coulomb collisions takes less than several picoseconds. Therefore, the fundamental principle of laser-material interaction changes when the pulse duration is significantly shorter than the energy transfer time. The ultra-short pulse duration (< 10 ps) implies that the conventional hydrodynamics motion does not to occur.

Ion separation is the third step of ablation. There are two forces which are momentum transfer from energetic electrons to the ions in the irradiated area. These two forces, electrostatic force and ponderomotive force, pull parent ions in opposite directions. The energetic electrons escape the material and create a strong electric field due to charge separation with the parent ions. The magnitude of this electric field ($\boldsymbol{E_a}$) depends on the electron kinetic energy $\varepsilon_e \sim (T_e - \varepsilon_{esc})$ (ε_{esc} is the work function) and on the gradient of the electron density along the normal to the target surface. This electric field of charge separation pulls out parent ion. This force is called the electrostatic force ($\boldsymbol{F_{el-st}}$). The electrostatic force can be evaluated by Debye length, $l_D \sim \nu_e/\omega_{pe}$, where $\nu_e = [(T_e - \varepsilon_{esc})/m_e]^{1/2}$ is the electron thermal velocity. $\boldsymbol{n_e}$ is the density of electron, $\boldsymbol{l_s}$ is the skin depth, ω_{pe} is the electron plasma frequency [Gamaly *et al.*, 2002].

$$E_a = -\frac{\varepsilon_e(t)}{e}\frac{\partial \ln n_e}{\partial z} \quad (6)$$

$$F_{el-st} = eE_a = -\varepsilon_e(t)\frac{\partial \ln n_e}{\partial z} \cong \frac{It}{nl_s l_D} \quad (7)$$

The ponderomotive force ($\boldsymbol{F_{pf}}$) is another force applied to the ions push into the material, so the parent ions are accelerated into the material. This force is a nonlinear force that a charged particle experiences in an inhomogeneous oscillating electric field. e is the an electric charge, m_e is the mass of electron.

$$F_{pf} = -\frac{2\pi e^2}{m_e c\omega^2}\nabla I \cong \frac{I}{2n_e c l_s}\frac{\omega_{pe}^2}{\omega^2} \tag{8}$$

Let us compare the force in the electrostatic field of the space charge to the ponderomotive force of the laser.

$$\left|\frac{F_{el-st}}{F_{pf}}\right| \cong 2\omega t_p\left(\frac{\omega}{\omega_{pe}}\right)\left(\frac{c}{v_e}\right) \tag{9}$$

For a solid state density plasma, $\omega_{pe}/\omega \sim 10$, the ratio is much more than 1, so the ponderomotive force can be neglected. The force of electrostatic field pulls the ions out of the material if the electron energy is larger than the binding energy of ions in the lattice.

3.2 Define DPs from Ablation Formulas

The design parameters of LED dicing machine are deducted based on the pulse-material interaction formulas. From Eq. (1) ~ (9), we can determine laser parameters (repetition rate, intensity, pulse duration, wavelength, and polarization state), which can be defined as design parameters of dicing machine.

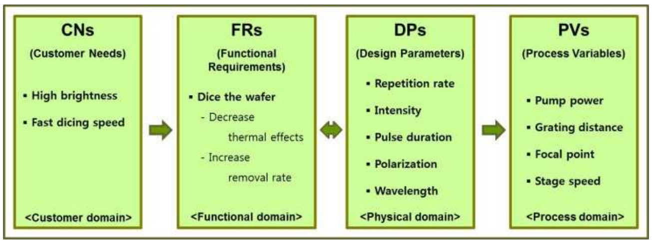

Figure 5. Design parameter of dicing machine.

FRs and DPs of novel LED dicing machine using ultra-short femtosecond pulse laser can be summarized as below.

FR1 = Dice the wafer
FR11 = Decrease thermal effects
FR12 = Increase dicing speed
DP1 = Repetition rate
DP2 = Intensity
DP3 = Pulse duration
DP4 = Polarization
DP5 = Wavelength

The design equation for the novel dicing machine can be written as

$$\begin{bmatrix} FR11 \\ FR12 \end{bmatrix} = \begin{bmatrix} x_{11} & x_{12} & x_{13} & x_{14} & x_{15} \\ x_{21} & x_{22} & x_{23} & x_{24} & x_{25} \end{bmatrix} \begin{bmatrix} DP1 \\ DP2 \\ DP3 \\ DP4 \\ DP5 \end{bmatrix} \tag{10}$$

3.3 Define Boundary Conditions of DPs

As a boundary condition of DPs, the ablation threshold (F_{th}, [Joule]) of the LED wafer described by the interaction between ultrafast fs laser pulse and material can be used [Gamaly *et al.*, 2002].

$$F_{th} = \frac{3}{4}(\varepsilon_b + J_i)\frac{l_s n_e}{A} \approx \frac{3}{4}(\varepsilon_b + J_i)\frac{c n_e}{2\omega} \tag{11}$$

The threshold of quartz wafers is about 1 J/cm^2, which implies that the pulse energy should exceed 1 µJ at 100 µm^2 focal area. Two DPs, the repetition rate and intensity, are related to the pulse energy.

Another boundary condition can be derived from the second step of the ablation mechanism as the pulse duration. To suppress heat transfer to the lattice, the pulse duration should be significantly shorter than the energy transfer time ~10 ps.

4 DPs Contributions to FRs

Each DP contributes to the FRs in a positive or negative manner. The tendency should be figured out here for DPs to be optimized to satisfy the FRs. Repetition rate means the frequency number of pulses per unit time (1 sec). The time interval between pulses becomes shorter as the repetition rate increases. If fs pulses are separated by several milliseconds, the temperature of the focal volume returns to room temperature before the next pulse arrives [Gattass *et al.*, 2006]. On the other hand, as the repetition rate increases, the pulse energy accumulates in the focal volume, which produces thermal structural changes, as shown in Figure 6. Therefore, we can conclude the higher repetition rate gives negative effects to the first FR (decrease thermal effects). However, the energy to ablate the target material increases with higher repetition rate, which gives positive effects to the second FR (increase dicing speed).

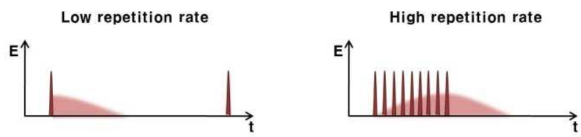

Figure 6. Energy deposits according to repetition rate.

The second DP is the intensity of the fs laser. The higher intensity ablates the target material more, which means that the intensity provides a positive effect on the second DP. Figure 7 shows various intensities and ablation thresholds. The higher intensity (①) offers more area exceeding the threshold but also a larger area below the threshold intensity.

Because the area below the threshold contributes to thermal effects, the high intensity can negatively affect FR1.

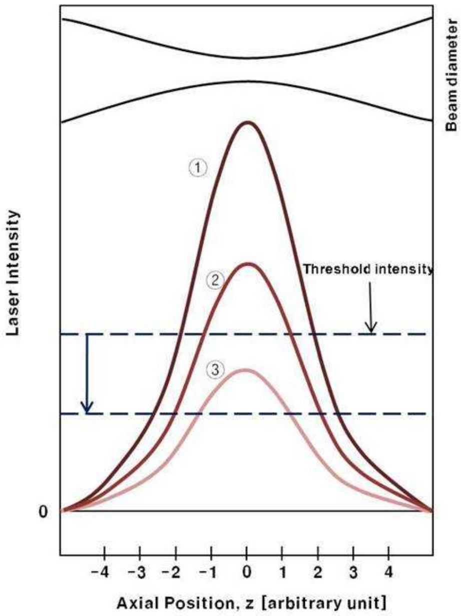

Figure 7. Time-dependent intensity in the focal region.

The third DP is the pulse duration, the temporal width of the pulse. As mentioned in section 3, a pulse duration that is shorter than the time needed for heat transfer from electron to lattice suppresses the heat increase in the lattice, which helps to satisfy FR1. Because the peak power is inversely proportional to the pulse duration, a shorter pulse duration offers a higher peak power. The threshold intensity for ablation decreases according to the decrease of the pulse duration as shown in Figure 7 [Giguere *et al.*, 2007]. As the pulse duration increase, the positive area of exceeding the threshold increases and the negative-effect area not exceeding the threshold also decreases. Therefore, a decrease of the pulse duration positively affects both FRs.

The polarization is the fourth DP. It was already shown in Eq. (5) that a circular polarization state is the most appropriate for efficient ionization. The fifth DP is the wavelength. The ablation threshold is inversely proportional to the wavelength of the laser, therefore a shorter wavelength gives us better performance for both FRs..

$$\begin{bmatrix} FR11 \\ FR12 \end{bmatrix} = \begin{bmatrix} - & - & - & + & - \\ + & + & - & x & - \end{bmatrix} \begin{bmatrix} DP1 \\ DP2 \\ DP3 \\ DP4 \\ DP5 \end{bmatrix} \qquad (12)$$

The DPs contribution tendencies to the FRs are summarized in Eq. (12). Repetition rate and intensity give contrary effects to each FR, although pulse duration and wavelength gives same ones. Therefore, to satisfy both FRs, we should shorten the pulse duration and wavelength in use. For repetition rate and intensity, it is essential to find out the detailed relationship between the FRs and DPs by using a theoretical and experimental approach

5 CONCLUSION

In conclusion, an ultra-fast fs laser based non-thermal LED dicing machine is designed by using an axiomatic design approach. We defined the CNs as 'high brightness' and 'fast dicing speed', and the FRs as 'decrease thermal effects' and 'increase dicing speed'. Through a detailed investigation about the interaction between ultrafast fs laser pulses and the target material, DPs are deduced. The DPs' contribution to each FRs is then visited. As a result, the repetition rate and intensity are shown to give contrary effects to each FR, whereas other DPs, pulse duration and wavelength, give the same. Further theoretical and experimental study is required to find optimal design to satisfy the FRs. It is anticipated that the proposed design approach would work for diverse next generation non-thermal processing of high value products with the finest structure and high processing speed.

6 REFERENCES

[1] Chichkov. B.N., Momma. C., Nolte. S., Alvensleben. F, Tunnermann. A., "Femtosecond, picosecond and nanosecond laser ablation of solids", *Appl. Phys. A*, Vol. 63, No. 2, pp. 109-115, 1996

[2] Gamaly. E.G., Rode. A.V., Luther-Davies. L., "Ablation of solids by femtosecond lasers: Ablation mechanism and ablation thresholds for metals and dielectrics", *Physics of Plasma*, Vol. 9, No. 3, pp. 949-957, 2002

[3] Gattass. R.R., Cerami. L.R., Mazur. E., "Micromachining of bulk glass with bursts of femtosecond laser pulses at variable repetition rates", *Optics Express*, Vol. 14, No. 12, 2006

[4] Giguere. D., Olivie. G., Vidal. F., Teotsch. S., Girard. G, Ozaki. T., Kieffer. J.C., "Laser ablation threshold dependence on pulse duration for fused silica and corneal tissues: experiments and modelling", *J. Opt. Soc. Am. A*, Vol. 24, No. 6, pp. 1562-1568, 2007

[5] Schaffer. C.B., Brodeur. A., Mazur. E., "Laser-induced breakdown and damage in bulk transparent materials induced by tightly focused femtosecond laser pulses", *Meas. Sci. Technol.*, Vol. 12, pp. 1784-1794, 2001.

[6] Suh N.P., *Axiomatic Design: Advance and Applications*, Oxford University Press, 2001